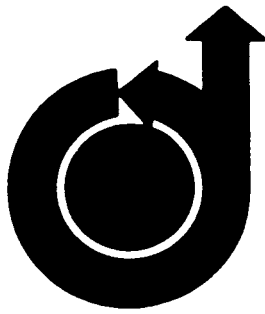


AIAA
TP
73-229



8p

**AIAA Paper
No. 73-229**

RECEIVED
A.I.A.A.
73 JAN -4 AM 9:26
T. I. S. LIBRARY

A73-16954

LONG-RANGE ENERGY-STATE MANEUVERS FOR
MINIMUM TIME TO SPECIFIED TERMINAL CONDITIONS

by
M. G. PARSONS
University of Michigan
Ann Arbor, Michigan
A. E. BRYSON, JR.
Stanford University
Stanford, California
and
W. C. HOFFMAN
Aerospace Systems, Incorporated
Burlington, Massachusetts

AIAA 11th Aerospace Sciences Meeting

WASHINGTON, D.C. / JANUARY 10-12, 1973

First publication rights reserved by American Institute of Aeronautics and Astronautics.
1290 Avenue of the Americas, New York, N. Y. 10019. Abstracts may be published without
permission if credit is given to author and to AIAA. (Price: AIAA Member \$1.50. Nonmember \$2.00).

Note: This paper available at AIAA New York office for six months;
thereafter, photoprint copies are available at photocopy prices from
AIAA Library, 750 3rd Avenue, New York, New York 10017

LONG-RANGE ENERGY-STATE MANEUVERS
FOR MINIMUM TIME TO SPECIFIED TERMINAL CONDITIONS*

M. G. Parsons**
University of Michigan

A. E. Bryson, Jr.†
Stanford University

W. C. Hoffman‡
Aerospace Systems, Inc.

A73-16954

Abstract

Some three-dimensional minimum-time paths to a specified line (or point), heading and energy are presented for an example supersonic aircraft. The optimum maneuvers have been determined using the calculus of variations and the energy-state approximation. These are compared with optimal solutions obtained with the additional assumption that only three discrete values of bank angle ($-\phi_{\max}$, 0 , $+\phi_{\max}$) are available. Constraints on thrust, Mach number, angle-of-attack, dynamic pressure, and load factor are included. For ranges long enough that maximum velocity is attained en route, the initial and final arcs can be determined separately, which greatly simplifies the solutions.

Nomenclature

- D = $D_0 + D_L \sec^2 \phi$ = aerodynamic drag; lb
 D_0 = $D_0(E, V)$ = zero-lift drag; lb
 D_L = $D_L(E, V)$ = drag due to $L = W$ at $\phi = 0$; lb
 E = $h + V^2/2g$ = energy height; ft
 L = $L_\alpha \alpha$ = aerodynamic lift; lb
 L_α = $L_\alpha(E, V)$ = lift curve slope; lb/deg
 M = V/a = Mach number
 T = thrust; lb
 V = velocity; ft/sec
 W = aircraft weight; lb
 a = local speed of sound; ft/sec
 g = gravitational acceleration; ft/sec²
 h = $E - V^2/2g$ = altitude; ft
 t = time; sec
 x, y = horizontal position coordinates; ft
 α = angle-of-attack; deg
 γ = $\sin^{-1}(h/V)$ = flight path angle relative to horizontal; deg
 ϕ = bank angle; deg
 ψ = heading angle; deg

Subscripts

- f = final value
 max = maximum value
 0 = initial value

Introduction

Use of the energy-state approximation greatly simplifies the determination of optimal flight paths for aircraft with only a small reduction in accuracy (see e.g. refs. 1 and 2). For three-dimensional flight paths the energy-state model requires three control variables: thrust (T), bank angle (ϕ), and altitude (h). For paths to a line (see fig. 1a) the model uses only three state variables, energy (E), heading (ψ), and distance to the line (x). For paths to a point (see fig. 1b), an additional state variable is needed: lateral position perpendicular to the line connecting the initial and final points (y). The equations of motion and applicable constraints are summarized in the appendix.

If the initial range (x_0) is sufficiently large that maximum velocity (V_{\max}) is reached in transit, the minimum-time path to a line can be separated into two parts (see fig. 2a). First, the minimum-time path is found to a straight V_{\max} arc perpendicular to the line (i.e. $\psi = 0$). Second, the minimum-time turn from the V_{\max} arc to the line is determined. The length of the intermediate V_{\max} arc then is obtained such that the sum of the ranges traversed on the three segments equals x_0 .

This "separation of arcs" greatly simplifies the solution since the initial-arc problem has only two parameters (E_0, ψ_0) and the final-arc problem has only two parameters (E_f, ψ_f). Each of these two problems can be solved by generating a one-parameter family of arcs. However, for short ranges (no V_{\max} arc) the problem has five parameters ($E_0, \psi_0, x_0, E_f, \psi_f$), and the tabulation of solutions is virtually impossible.

The arcs can also be separated, for sufficiently long range, in determining minimum-time paths to a point (see fig. 2b). However, in addition to the length of the V_{\max} arc, its heading and its intercept distance

* This research was supported by: ONR Contract N00014-67-A-0112-0063, Work Unit NP 213-085; NASA Grant 05-020-007; and AFOSR Contract F44620-72-C-0001.

** Assistant Professor, Department of Naval Architecture and Marine Engineering.

† Professor and Chairman, Department of Aeronautics and Astronautics; Fellow, AIAA; Consultant and Director, Aerospace Systems, Inc.

‡ Project Engineer.

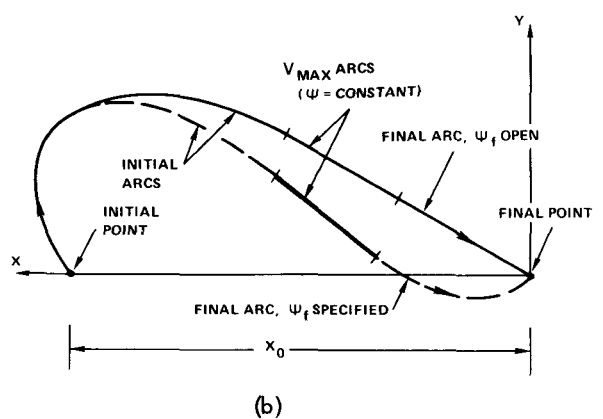
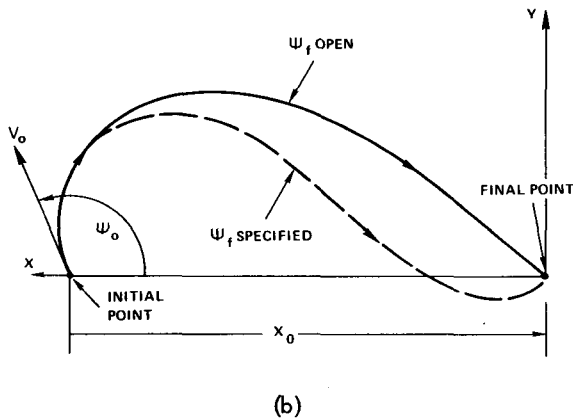
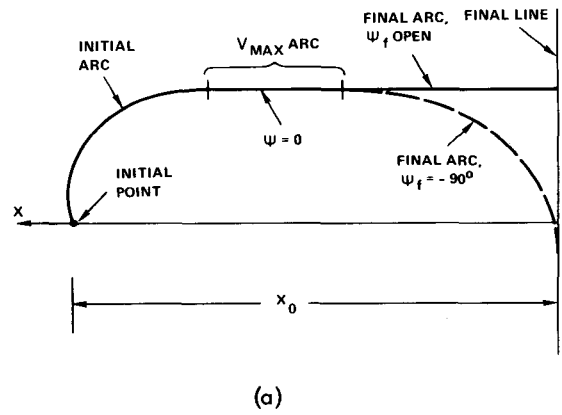
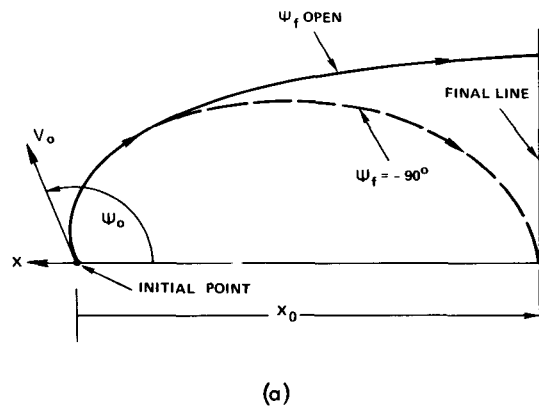


Figure 1. Horizontal Projection of Flight Paths (a) to a Line and (b) to a Point.

Figure 2. Horizontal Projection of Minimum-Time Paths (a) to a Line and (b) to a Point.

(x coordinate where V_{max} arc or its extension intercepts $y = 0$) must also be determined. This can be done iteratively using the two-parameter families of initial and final arcs mentioned previously.

Aircraft Flight Envelope for Zero Bank Angle

Figure 3 shows the flight envelope of an early F4 ("Phantom") airplane at weight (W) of 35,000 lb for zero bank angle ($\phi = 0$) and lift (L) approximately equal to W (see reference 3 for thrust, lift, and drag data). The aircraft can move along constant energy contours ($E = \text{constant}$) very quickly by "zoom" dives or climbs (effected by changing angle-of-attack). The high-altitude, low-velocity limit of zoom climbs is the maximum angle-of-attack (α_{max}) boundary. Here we took $\alpha_{max} = 12^\circ$. The low-altitude, high-velocity limit of zoom dives is the maximum velocity (V_{max}) boundary or the zero altitude ($h = 0$) boundary. V_{max} is the maximum velocity independent of E . Also shown are the contours where drag (D) equals maximum thrust (T_{max}). These contours separate regions where $\dot{E} < 0$ and $\dot{E} > 0$ with $T = T_{max}$. Energy is charged by adjusting the thrust.* The region

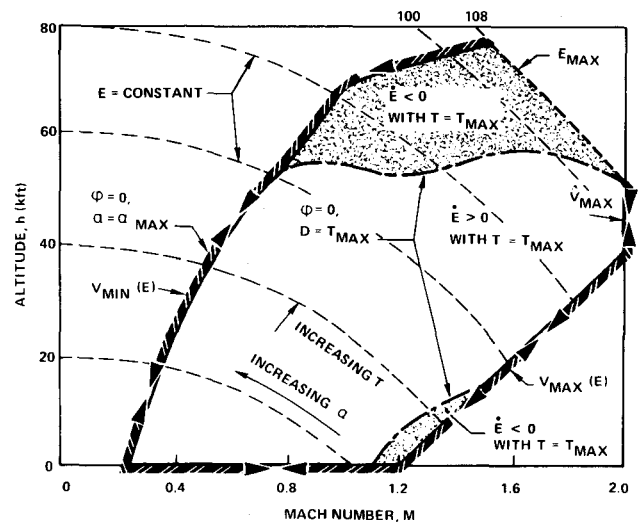


Figure 3. Aircraft Flight Envelope with $\phi = 0$, $L \approx W$.

* Note at low energies, the constant energy contours are almost parallel to constant altitude contours, so angle-of-attack primarily controls speed while thrust primarily controls altitude. At high energies, the constant energy contours are almost parallel to constant speed curves, so α primarily controls altitude while T primarily controls speed.

where $\dot{E} > 0$ with $T = T_{max}$ is quite large and extends up to $E = E_{max} = 108$ kft.

Minimum-Time Paths to a Given Long Range: $\psi_0 = 0$,
 ψ_f Unspecified

Figure 4 shows the altitude-Mach number profile of flight paths that yield minimum time to a given long range when no turning or slowing-down is required ($\psi_0 = 0$, ψ_f unspecified). ("Long range" will be used henceforth to indicate that a V_{max} arc occurs on the path). An example is indicated for $E_0 = E_f = 3$ kft. For other values of E_0 and E_f , zoom maneuvers at constant E to the ascent path

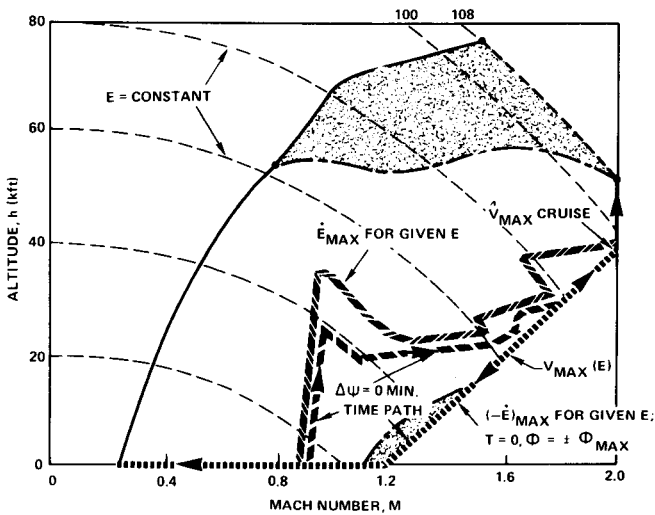


Figure 4. Altitude-Mach Number Profile of $\psi = 0$ Path for Minimum Time to a Given Long Range.

and from the descent path are used. The ascent ($\dot{E} > 0$) path uses $T = T_{max}$ but is not the same as the path for maximum \dot{E} (also shown in Figure 4). The $\psi = 0$ minimum-time path has higher velocity at each energy level than the $(\dot{E})_{max}$ path (see ref. 1). The descent path is along the $V_{max}(E), (-\dot{E})_{max}$ boundary using $T = 0$ and "chatter", i.e. banking rapidly first to ϕ_{max} , then to $-\phi_{max}$, in order to maximize the drag due to lift ($L = W \sec \phi_{max}$).

Figure 5 shows the altitude-range profile of the flight paths in Figure 4. For long ranges, the initial and final arcs are determined separately; a V_{max} cruise arc is inserted between them with appropriate range so that the total range is the specified x_0 . For example, with $E_0 = E_f = 40$ kft, any range greater than 88 nm will include an initial arc of 80 nm range, a V_{max} arc and a final arc of 8 nm range.

Aircraft Flight Envelope for Maximum Bank Angle Turning

Figure 6 shows the flight envelope of the same airplane in turning maneuvers at maximum bank angle ($\phi = \phi_{max}$), with $L \cos \phi_{max} = W$, i.e. the vertical component of lift equal to weight. Here we took $\tan \phi_{max} =$ maximum load factor = 4. The maximum angle-of-attack boundary is also the locus of maximum turn-rate ($\dot{\psi}_{max}$) and minimum velocity for a given energy ($V_{min}(E)$). This boundary is now substantially lower than in Figure 3, as is the contour where $D = T_{max}$. The intersection of these two contours at $h = 20$ kft, $M = .75$ is the highest energy where maximum turn rate can be sustained (called the

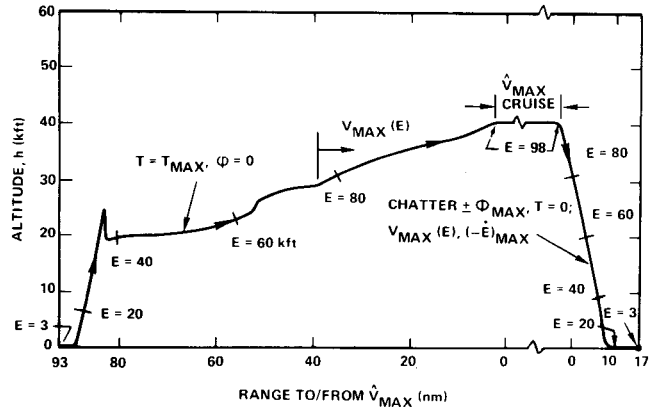


Figure 5. Altitude-Range Profile $\psi = 0$ Path for Minimum Time to a Given Long Range.

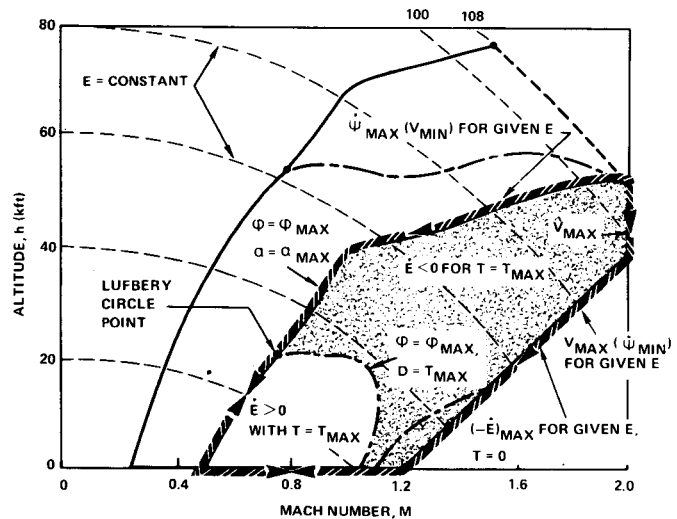


Figure 6. Aircraft Flight Envelope for $\phi = \phi_{max}$, $L \cos \phi_{max} = W$.

Lufbery circle point in ref. 4). The region where $\dot{E} > 0$ with $T = T_{max}$, $\phi = \phi_{max}$ is relatively small and occurs in the transonic speed regime below $h = 20$ kft.

Minimum-Time Paths to a Line (Long Range): $\psi_0 \neq 0$,
 E_f and ψ_f Unspecified

Figure 7 shows a horizontal projection of a typical minimum-time path to a given line which is far enough away that a V_{max} cruise arc occurs en route. The case shown is for $E_0 = 43$ kft, $\psi_0 = 180^\circ$. The continuous bank angle solution (ref. 5) uses a ψ_{max} turn for the first 110° (to $\psi = 70^\circ$), then a gradually decreasing altitude and bank angle to the $\Delta\psi = 0$ minimum-time locus of Figure 4. Note that $\psi = 0$ is not reached "exactly" until $V = V_{max}$ at a range of 86 nm. Also shown in Figure 7 is a suboptimal path with ϕ limited to three discrete values

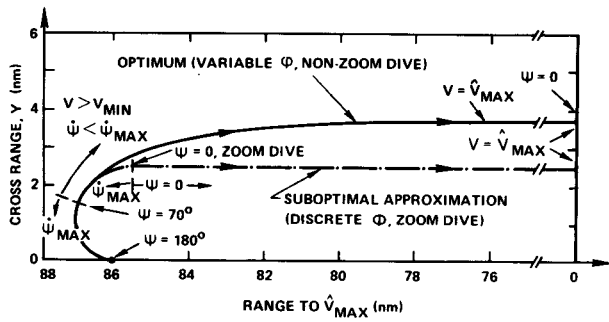


Figure 7. Horizontal Projection of a Typical Minimum-Time Turn to a Given Long Range, $E_0 = 43$ kft.

($-\phi_{max}, 0, +\phi_{max}$). It consists of a $\dot{\psi}_{max}$ turn all the way to $\psi = 0$ (which occurs at a range of 0.5 nm), then a zoom dive to the $\Delta\psi = 0$ minimum-time locus of Figure 4. Both paths reach V_{max} at substantially the same time and distance (86 nm). Because of its simplicity, this suboptimal path provides a significant reduction in computational requirements, with only a slight reduction in flight time. This model appears to be quite similar to the energy-maneuverability model of Boyd (ref. 6).

There are four types of minimum-time turns to a given long range where E_f and ψ_f are unspecified. Figure 8 shows the accelerating turn case where $E_0 <$

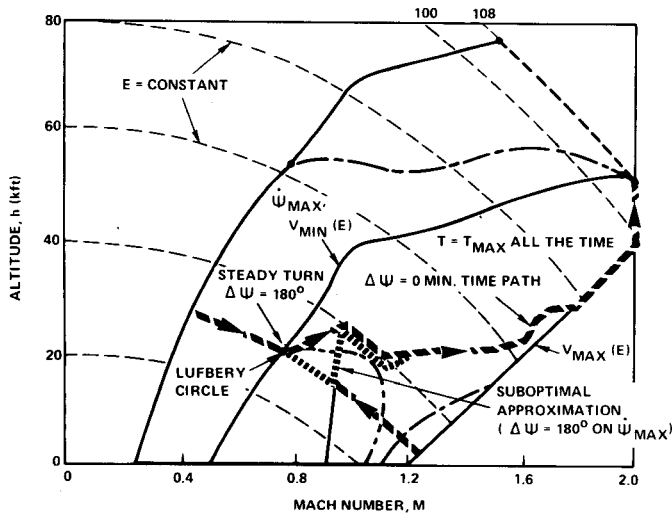


Figure 8. Minimum-Time Turns to a Given Long-Range (E_f, ψ_f Unspecified), $E_0 < 30$ kft.

30 kft. For $\psi_0 = 0$, the aircraft zoom dives to $h = 0$ and follows the $\Delta\psi = 0$ minimum-time path. For $0^\circ < \psi_0 \leq 180^\circ$, the aircraft zoom dives or climbs to the $\dot{\psi}_{max}$ locus where an accelerating turn takes place, followed by a zoom dive to the $\Delta\psi = 0$ minimum-time path. Figure 9

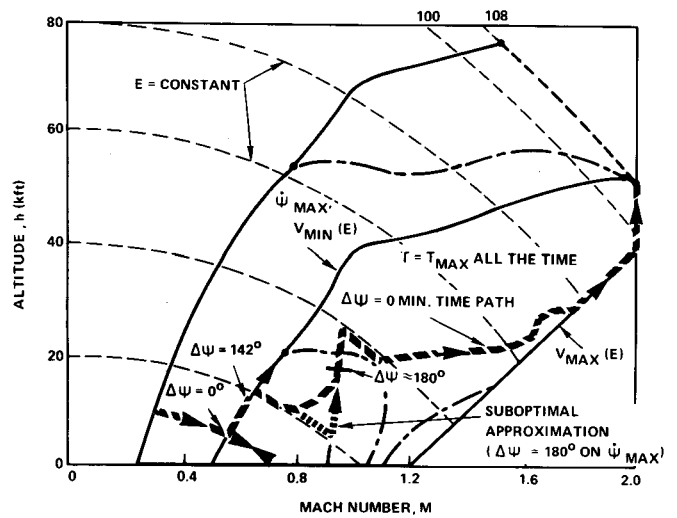


Figure 9. Minimum-Time Turns to a Given Long Range (E_f, ψ_f Unspecified), $E_0 = 30$ kft.

shows the constant-velocity turn case where $E_0 = 30$ kft. Here the aircraft zoom dives or climbs to the $\dot{\psi}_{max}$ locus where a constant-velocity turn takes place, followed by a zoom dive to the $\Delta\psi = 0$ minimum-time path. Figure 10 shows a decelerating turn case where $30 \text{ kft} < E_0 < 93$ kft. The aircraft zoom dives or climbs to the $\dot{\psi}_{max}$ locus where a decelerating turn takes place, followed by a zoom dive

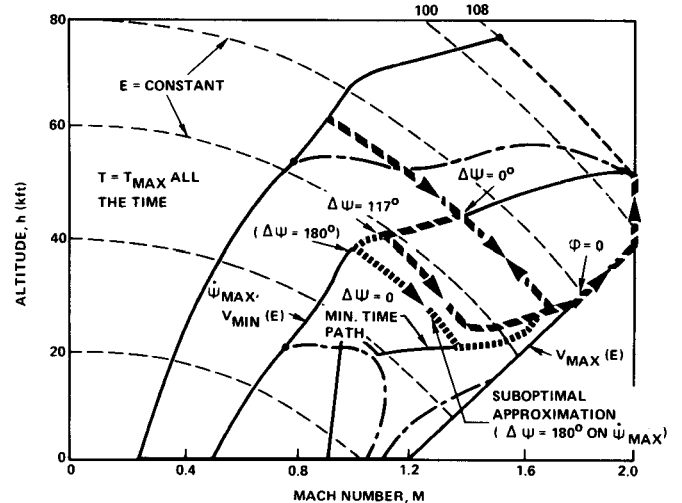


Figure 10. Minimum-Time Turns to a Given Long Range (E_f, ψ_f Unspecified), $30 \text{ kft} < E_0 < 93$ kft.

to the $\Delta\psi = 0$ minimum-time path. The examples of Figures 8-10 all used $T = T_{max}$. For $E_0 > 95 + (180 - \psi_0/13)$ kft, an initial period of $T = 0$ is required. An example of such a case is shown in Figure 11 for $E_0 = E_{max} = 108$ kft and

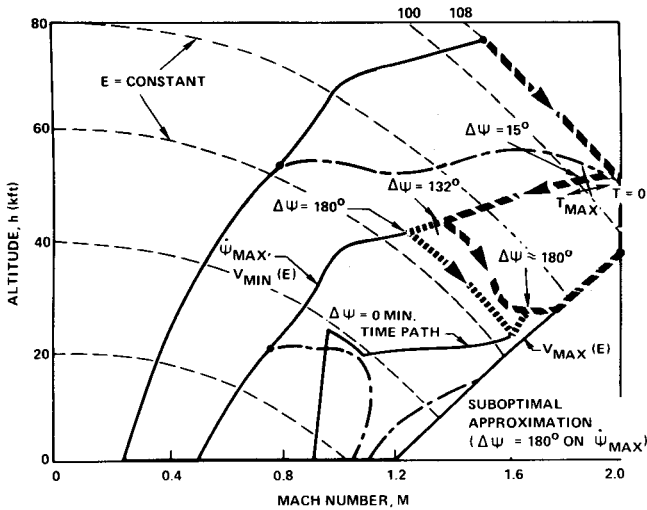


Figure 11. Minimum-Time 180° Turn to a Given Long Range (E_f, ψ_f Unspecified), $E_0 = E_{max} = 108$ kft.

$\psi_0 = 180^\circ$. The aircraft turns about 15° before T is switched from zero to T_{max} to complete the turn.

Figure 12 shows all minimum-time turns to a given long range (E_f, ψ_f unspecified) with E_0, ψ_0 as parameters. Note there is a range of possible E_f from 98 to 108 kft at $\dot{\psi}_{max}$. The suboptimal paths with a $\dot{\psi}_{max}$ turn all the way to $\psi = 0$, then a zoom dive to the $\Delta\psi = 0$ minimum-time path are also depicted.

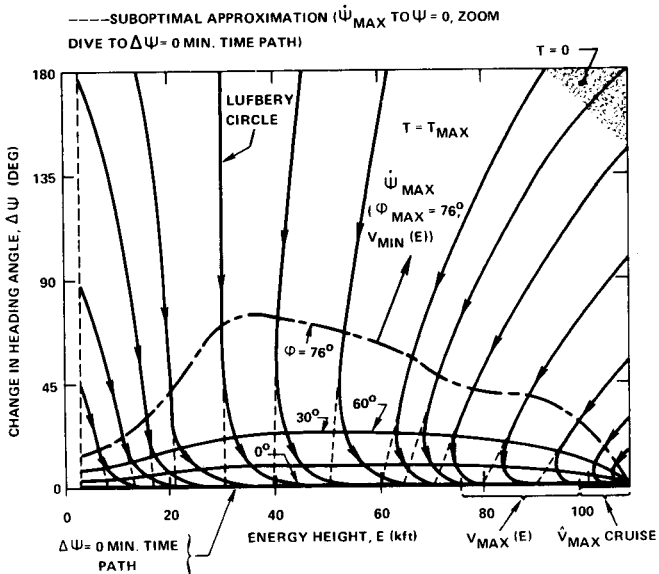


Figure 12. Minimum-Time Turns to a Given Long Range (E_f, ψ_f Unspecified).

Minimum-Time Flight Paths to a Point or Line from V_{max} Cruise; E_f and ψ_f Specified

Figures 13 and 14 show a horizontal projection and an h vs M profile, respectively, of a typical minimum-time path to a point or line from V_{max} cruise. The case

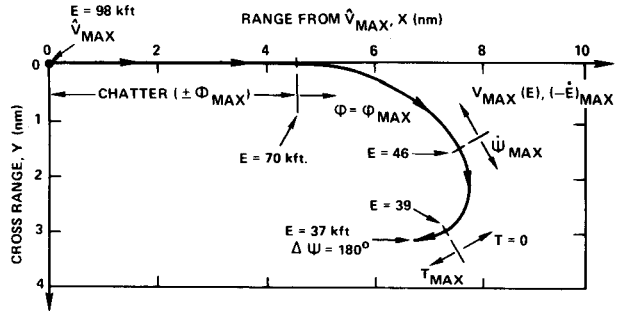


Figure 13. Horizontal Projection of Typical Minimum-Time Path to a Point from V_{max} Cruise.

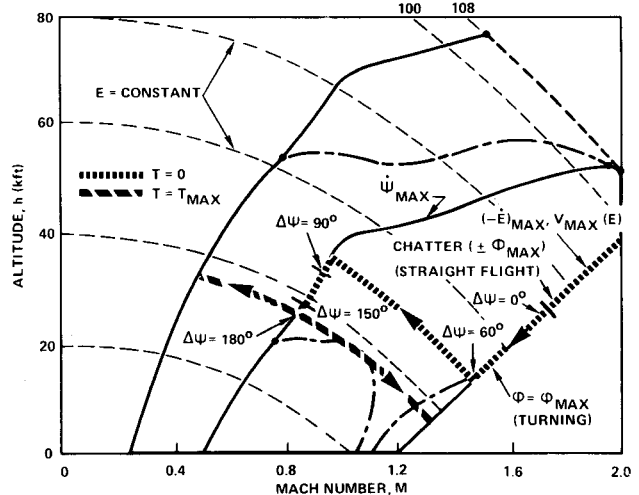


Figure 14. Minimum-Time 180° Turn to a Point from V_{max} Cruise, $E_f = 37$ kft.

shown is for $E_f = 37$ kft, $\Delta\psi = 180^\circ$. It consists of: (a) a straight chatter arc ($\phi = \pm \phi_{max}$) descending in altitude on the $V_{max}(E)$ boundary with $T = 0$ to $E = 70$ kft; (b) a ϕ_{max} turn, still descending on the $V_{max}(E)$ boundary with $T = T_{max}$, to $\Delta\psi \approx 60^\circ$, $E \approx 47$ kft; (c) a zoom climb to the $\dot{\psi}_{max}$ boundary; (d) a $\dot{\psi}_{max}$ turn, decelerating with $T = 0$, to $\Delta\psi = 150^\circ$, $E \approx 39$ kft; (e) a $\dot{\psi}_{max}$ turn decelerating with $T = T_{max}$, to $\Delta\psi = 180^\circ$, $E_f = 37$ kft; and finally (f) a zoom climb or dive to the desired final altitude. Note this same case applies to turning onto a line ($\Delta\psi = \pm 90^\circ$) if $E_f \approx 44$ kft (there would be no $T = T_{max}$ phase).

Figure 15 shows another type of path for $E_f = E_{max} = 108$ kft, $\Delta\psi = 180^\circ$. It uses $T = T_{max}$ all the way and

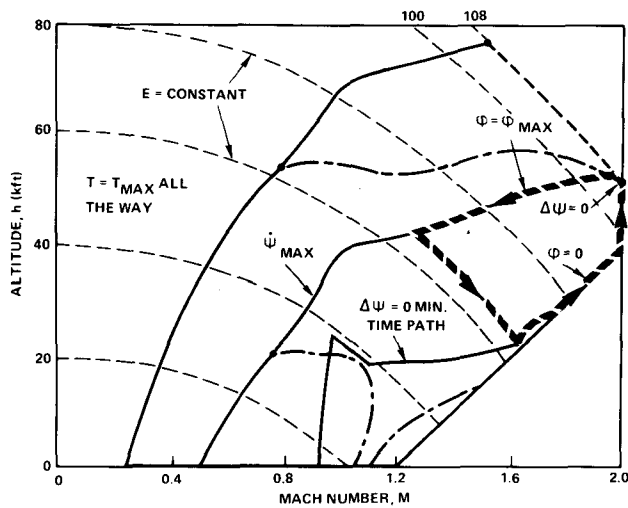


Figure 15. Minimum-Time 180° Turn to a Point from \dot{V}_{max} Cruise, $E_f = E_{max} = 108$ kft.

consists of four arcs: (a) $\dot{\psi}_{max}$ turn decreasing energy to 67 kft and turning 180°, (b) a zoom dive to the $\Delta\psi = 0$ minimum-time path, (c) with $\phi = 0$, moves along $\Delta\psi = 0$ minimum-time path to the $V_{max}(E)$ boundary, up that boundary to $M = 2$, and (d) a constant Mach number climb at $M = 2$ to $E_f = 108$ kft.

Figure 16 shows all minimum time turns to a point or line from \dot{V}_{max} cruise with $E_f, \Delta\psi_f$ as parameters. Note that paths may start anywhere on $\Delta\psi = 0$, $98 < E < 108$ assuming that the appropriate energy would have been achieved during the cruise by a constant Mach climb.

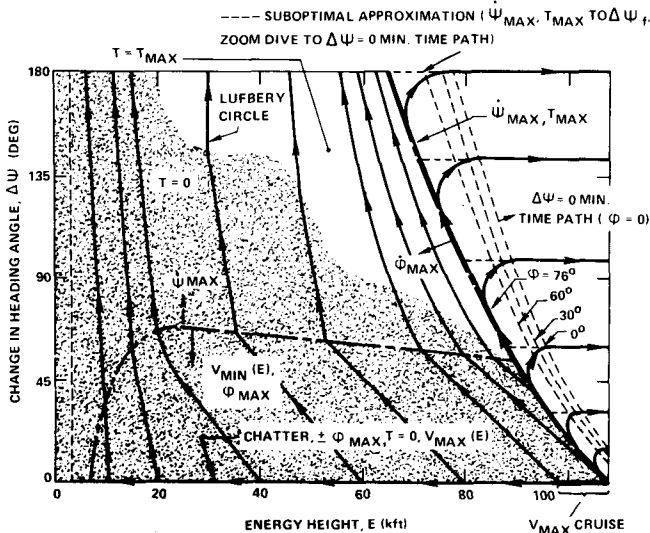


Figure 16. Minimum-Time Turns to a Point or Line from \dot{V}_{max} Cruise.

Paths that Reach $V_{max}(E)$ but not \dot{V}_{max}

It is also possible to "separate arcs" for cases where the initial turn reaches $V_{max}(E)$ but not necessarily \dot{V}_{max} with $\phi = 0$. It is only necessary to match E_f of the initial arc to E_0 of the final arc where, in this case, $75 \leq E \leq 98$ kft.

Conclusions

When the initial range is sufficiently large that the maximum velocity constraint is encountered en route, the calculation of minimum-time maneuvers can be greatly simplified by a separation of arcs into two 2-parameter problems. For shorter ranges the solution involves five parameters. Suboptimal paths along which the bank angle is restricted to three discrete values ($-\phi_{max}, 0, +\phi_{max}$) compare favorably with the optimum, continuous bank angle solutions for transonic speeds and below. At very high speeds the difference becomes more noticeable. However, the suboptimal paths are much simpler to compute and increase the flight time only moderately, thus making them attractive for possible on-line, real-time applications.

References

1. Bryson, A. E., Jr., Desai, M. N. and Hoffman, W. C., "Energy-State Approximation in Performance Optimization of Supersonic Aircraft", Journal of Aircraft, Vol. 6, No. 6, November-December 1969, pp. 481-488.
2. Hedrick, J. K. and Bryson, A. E., Jr., "Three-Dimensional, Minimum-Time Turns for a Supersonic Aircraft", Journal of Aircraft, Vol. 9, No. 2, February 1972, pp. 115-121.
3. Parsons, M. G. and Bryson, A. E., Jr., "Three-Dimensional, Minimum-Time Flight Paths to a Point and Onto a Line for a Supersonic Aircraft with a Maximum Mach Number Constraint", Paper No. 32-4, 1972 Joint Automatic Control Conference, Stanford University, August 16-18, 1972.
4. Kelley, H. J. and Lefton, L., "Supersonic Aircraft Energy Turns", Presented at the Fifth IFAC Congress, Paris, France, June 12-17, 1972.
5. Parsons, M. G., "Three-Dimensional, Minimum-Time Turns to a Point and onto a Line for a Supersonic Aircraft with a Maximum Mach Number Constraint", Ph.D. Dissertation, Department of Applied Mechanics, Stanford University, Stanford, California, July 1972.
6. Boyd, J. R., "Maximum Maneuver Concept", Informal Briefing, USAF Systems Command Headquarters, Andrews Air Force Base, Maryland, July 2, 1971.

Appendix — Equations of Motion and Constraints

The equations of motion for three-dimensional flight using the energy-state approximation are (see Nomenclature):

$$\dot{E} = \frac{V}{W} (T - D_0 - D_L \sec^2 \phi)$$

$$\dot{\psi} = \frac{g}{V} \tan \phi$$

$$\dot{x} = -V \cos \psi$$

$$\dot{y} = V \sin \psi$$

The state variables are E , ψ , x and y ; the three control variables are V , T and ϕ . The auxiliary variables h , α , and γ are defined in the Nomenclature. These equations assume: (a) $|\alpha| \ll 1$, $|\gamma| \ll 1$, (b) $V|\dot{\gamma}| \ll g$, (c) instantaneous velocity changes possible at constant E (zoom dives or climbs), (d) $T \ll L_\alpha$, and (e) weight change is negligible during the maneuver.

The following constraints are observed:

$$0 \leq T \leq T_{\max}(E, V)$$

$$V_{\min}(E, \phi) \leq V \leq V_{\max}(E)$$

$$-\phi_{\max} \leq \phi \leq +\phi_{\max}$$

where

$$T_{\max}(E, V) = \text{maximum available thrust}$$

$$\tan \phi_{\max} = \text{maximum permissible turning load factor (g's)}$$

The maximum velocity constraint is imposed by engine and dynamic pressure limits and the constraint that $h \geq 0$ (see Fig. 3). The minimum velocity constraint (see Figs. 3 and 7) results from specifying a maximum angle-of-attack:*

$$\alpha = \frac{W \sec \phi}{L_\alpha(E, V)} \leq \alpha_{\max}$$

The bank angle constraint assures that the crew are not subjected to excessively high load factors.**

* α_{\max} was taken as 12° for our examples.

** ϕ_{\max} was taken as $\approx 76^\circ$ for our examples ($\tan \phi_{\max} = 4$).